ORIGINAL PAPER

Small calcified coronary atherosclerotic plaque simulation model: minimal size and attenuation detectable by 64-MDCT and MicroCT

Wisnumurti Kristanto · Peter M. A. van Ooijen ·
Jaap M. Groen · Rozemarijn Vliegenthart ·
Matthijs Oudkerk

Abstract Zero calcium score may not reflect the absence of calcifications as small calcifications could be missed. This study aimed to evaluate minimal size and minimal attenuation of coronary calcifications detectable by computed tomography (CT) and to determine the minimal spatial resolution required for detecting calcification onset. Using open source CT simulation software, CTSim$^{©}$, several 50%-stenotic coronary artery phantoms were designed with 5 μm resolution, realistic morphology and tissue-specific Hounsfield Unit (HU) values. The plaque had an attenuation resembling fibrous plaque and contained a single calcification. X-ray projections were simulated with settings resembling non-contrast-enhanced 64 multi detector-row CT (64-MDCT). Scanning and reconstruction were simulated with spatial resolution of a 64-MDCT (0.4mm) and of a MicroCT (48 μm). Starting from a single calcium granule, the calcification was simulated to grow in size and attenuation until it could be detected using clinically accepted calcium determination scheme on MicroCT and 64-MDCT images. The smallest coronary calcifications detectable at MicroCT and 64-MDCT, which had a realistic attenuation (−1,024 to 3,072 HU), were of 25 μm and 215 μm diameter, respectively. The area was overestimated 7.7 and 8.8 times, respectively. Calcifications with smaller size need to have an unrealistically high attenuation to be detectable by 64-MDCT. In conclusion, 64-MDCT is only able to detect coronary calcifications with minimal diameter of 215 μm. Consequently, early onset of calcification in coronary plaque will remain invisible when using CT and a zero calcium score can not exclude the presence of coronary calcification.

Introduction

Computed tomography (CT) is highly sensitive for the detection of coronary calcification, due to the high attenuation value of calcium. Using this property, it has been shown in multiple large prospective studies that the amount of coronary calcification, expressed as a calcium score [1], is a strong predictor of coronary events [2–4]. Therefore, the calcium score is considered a promising method to improve cardiovascular risk stratification [5–7]. Furthermore, the occurrence of coronary heart disease and mortality is extremely unlikely in asymptomatic individuals with a zero or very low calcium score [8, 9].

W. Kristanto (✉) · P. M. A. van Ooijen ·
J. M. Groen · R. Vliegenthart · M. Oudkerk
Department of Radiology, University Medical Center
Groningen, University of Groningen, Hanzeplein 1,
P.O. BOX 30001, 9700RB Groningen, The Netherlands
e-mail: w.kristanto@rad.umcg.nl

However, whether the absence of coronary calcium can also exclude the presence of obstructive plaque in patients with symptoms suggesting underlying coronary artery disease (CAD) is a matter of debate. In different studies with differing CT systems, the presence of significant stenosis on CT angiography in case of a zero calcium score ranged from 0 to 7% [10–14]. Although some authors have suggested that the zero calcium score can reliably exclude the presence of obstructive disease, others advise to be careful with patients with zero calcium score due to the inability to rule out CAD [13–15]. It should be proven that a zero calcium score on CT indeed means that coronary calcification is absent and that significant CAD can be safely excluded. The inability to detect small and less dense calcifications was shown in a recent phantom study, in which coronary calcification quantifications were compared between multiple 64 multidetector-row CT (MDCT) scanners from two different vendors [16].

The current MDCT technology has limited spatial resolution to detect small calcifications. Therefore, by using a software simulation model, we investigated the smallest calcification which can be detected by current CT technology and the spatial resolution needed to detect significant calcifications based on the commonly accepted HU-based threshold for calcification measurement in non-contrast-enhanced CT.

Materials and methods

The simulation was conducted using an open source CT simulation software package, CTSim© 3.0 [17, 18]. The simulation was started by generating a custom-made phantom. Hereafter, X-ray projections on the phantom were simulated, and the resulting sinogram was reconstructed to make the final CT image.

Phantom generation

The phantom depicts an axial cross-section of a coronary vessel and was generated at 5 μm resolution to facilitate the smallest size of a single calcium granule, found in histopathology [19]. Realistic morphological features of the vessel and attenuation values of the tissues and materials were used [20–28].

All three layers (intima, media, and adventitia) of a coronary vessel and the surrounding epicardial fat tissue were incorporated into the design of the phantom. Published attenuation values of carotid plaques were chosen. Although the studies reporting these values used contrast-enhanced CT scans, carotid plaques are generally large enough to be less influenced by partial volume effects, either from the lumen contrast-enhancement or the surrounding fat tissue. The lumen was simulated to be blood-filled, while both the normal and plaque-infested parts of the vessel were fibrous. The plaque was designed to build up in the intima area causing 50% area stenosis with a single calcification inside. The construction and dimension of the phantom is presented in Fig. 1a.

Scanning simulation

X-Ray projections were simulated on the generated phantom and performed with settings based on the technical specifications of a commercially available 64-MDCT scanner (Somatom Sensation 64, Siemens Medical Solution, Forchheim, Germany). This scanner was considered to be an appropriate representative of the current clinical CT systems used in cardiac imaging. The scan settings of 64-MDCT adapted to the simulation were: the scanning voltage, amount of projections to make one image slice, and spatial resolution. The generally used 120 kV voltage setting for coronary CT calcium scoring examinations was not directly simulated by the scanning parameters. Instead, since voltage settings affect the HU values of the scanned materials, it was simulated by taking the HU values for plaque tissues in the phantom construction from studies which used 120 kV scanning voltage setting. Per 180° rotation, 1,151 projections were made, resembling the number of projections made by 64-MDCT at 330 ms rotation time. Due to the limitation of the software, the geometry of the detectors was set to be parallel instead of equiangular (i.e. equal to fan beam geometry) to mimic the configuration of 64-MDCT X-ray source-detector. However, because of the relatively small size of the phantom in comparison to the distance between X-ray source and detector, a fan-beam ray passes through the phantom in a similar way as a parallel beam ray would and thus this will not influence the results. The detector array element size was set to be 0.4 mm, the spatial resolution of a 64-MDCT. The same projections were

Fig. 1 The vessel phantom (a) with fibrotic plaque and a single calcification was generated at 5 μm resolution. CT scanning simulation was conducted, generating images at MicroCT (b) and 64-MDCT (c) resolution
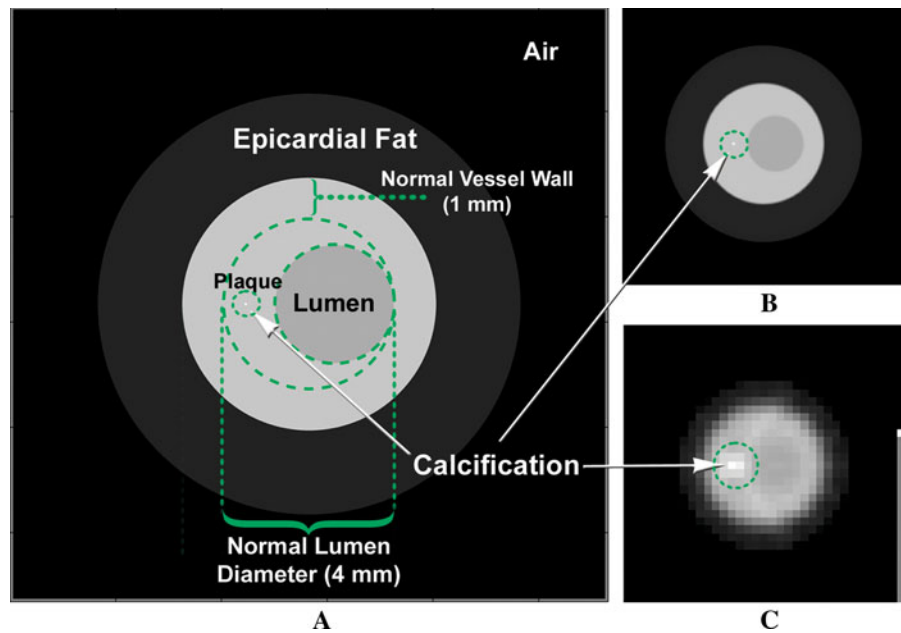
repeated with similar settings but with the detector array element size changed to 48 μm, the spatial resolution of a MicroCT system (Kristanto et al. European Society of Cardiac Radiology, Porto 2008). Inapplicable scan settings of 64-MDCT were the pitch and scanning time because the phantom was stationery, and the slice width because the phantom was two dimensional.

Two other variables of clinical scans which were indirectly incorporated in the simulation were the scan current and the scanning environment inside a thorax cage. Both are known to be related to noise, affecting image quality. Adhering to this fact, an artificial noise comparable to noise in clinical scans was incorporated at the later stage of the simulation.

Reconstruction parameters

From the resulting sinograms of the X-ray projections, images were reconstructed using the filtered back projection (FBP) method with a Hanning filter and linear interpolation. The Hanning filter was selected because of its smoothing characteristics, comparable to a medium or smooth kernel, usually applied for coronary CT calcium scoring examinations. The reconstructed image pixel size was set to 48 μm and 0.4 mm to match the MicroCT and 64-MDCT spatial resolutions, respectively (Fig. 1b, c).

The parameters used for simulation are summarized in Table 1.

Analysis

Since a calcification grows as several calcium granules aggregate [29], the calcification was systematically simulated to grow, starting from a single calcium granule, until it was detected by either 64-MDCT or MicroCT. The growth was simulated either by altering the attenuation value (by increasing the HU value) or the size (by increasing the diameter, assuming the granules aggregate in a circular shape), thus changing the physical properties of the calcification in the phantom images. Two parameters were investigated:

1. Minimal attenuation value of detectable calcification

The diameters of the calcifications were fixed into several predefined sizes: 1-, 2-, 3-, 5-, and 10-pixel (with 1 pixel = 5 μm = 1 calcium granule). At each fixed diameter, the attenuation value was increased from 130 HU until it was detected by either CT system.

2. Minimal size of detectable calcification

The second simulation assumed that calcium granules have a specific attenuation value. The attenuation value of an area will be the average of

Table 1 Parameters used for simulation

Phantom

  Element size: 5 μm

  Vessel morphology

    Normal wall thickness: 1 mm
(intima + media + adventitia); 0.5 mm (adventitia only)[a]

    Normal lumen diameter: 4 mm[b]

    Vessel shape: eccentric thickening with round lumen[c]

  Tissue attenuation value

    Air: −1,024 HU

    Blood: 50 HU[d]

    Epicardial fat: −100 HU[e]

    Fibrous plaque: 65 HU[f]

Scanning/X-ray projection

  Detector geometry: parallel

  Detector size: 48 μm/0.4 mm (MicroCT/64-MDCT)

  Number of projections: 1,151

Reconstruction

  Type of reconstruction: filtered back projection (FBP)

  Type of filter: hanning

  Interpolation: linear

  Pixel size: 48 μm/0.4 mm (MicroCT/64-MDCT)

[a] Normal coronary wall layers thickness (for all three layers and for adventitia layer only) [23], and then rounded for simplification

[b] Normal lumen diameter [20]

[c] The most common plaque-burdened vessel shape [20]

[d] Arbitrarily chosen from the normal range of the reported value for blood. [25]

[e] Arbitrarily chosen from the normal range used for epicardial fat [22, 27]

[f] Average of published carotid fibrous plaque values [21, 24, 26, 28], and then rounded for simplification

the attenuation value of all components in that area. As calcium granules aggregate and fill an entire pixel area, the attenuation value of the area will reflect the attenuation value of a single calcium granule. The attenuation value of this area will also be the highest since calcium is the densest plaque component. The maximum reported coronary calcification attenuation value was found to be approximately 2,000 HU [30]. Therefore, the attenuation value of the calcification was fixed at 2,000 HU, and then the diameter was increased starting from 1 pixel (with 1 pixel increments) until it was detected by either CT system.

The position of the calcification relative to the reconstructed image pixel borders may influence its

detectability as a calcification at the center of an image pixel is blurred less than a calcification at the border of two image pixels. Therefore, additional investigation was conducted by varying the position of the calcification relative to the reconstructed image pixel(s), both for 64-MDCT and MicroCT images, into three variations: at the center of an image pixel, at the border between two image pixels, and at the border between four image pixels (see Fig. 2).

Noise could hamper the image quality and subsequently the calcification's detectability. Artificial noise was incorporated into the simulation according to the method described in a previous publication [31], by adding Gaussian noise with zero mean and sigma (σ) standard deviation to the sinograms. The σ was set to a certain value so that the noise in the reconstructed image matched the noise in normal clinical CT images used for calcium scoring application. The normal clinical CT image sample was taken from a thorax phantom scan (QRM, Möhrendorf, Germany; see Fig. 3), scanned on a 64-MDCT scanner in sequential mode at 120 kV and 50 mAs; reconstructed using B35f kernel at 3 mm slice thickness. The noise was defined as the standard deviation inside an ROI over a homogenous area with attenuation equivalent to water. To achieve correct noise simulation in the micro CT simulation the noise has to be increased by a factor of $N\sqrt{N}$, where N corresponds to the increase in resolution when compared to 64MDCT [32]. The resolution of MicroCT was 8.3 times the 64-MDCT. Therefore, the noise in the MicroCT images is approximately 24 times the noise in the 64-MDCT images.

Each time the calcification's size, attenuation value, or position was changed, a new phantom was generated and a new simulation was conducted. Based on the known plaque area on the phantom image, a region of interest (ROI) was defined on all MicroCT and 64-MDCT images, enclosing the whole plaque area. Two calcification detection criteria were defined according to the clinically accepted threshold of 130 HU for the detection of calcified plaque regions in non-contrast-enhanced 64-MDCT: firstly, when there was 1 pixel and secondly, when there were more than (>) 1 pixel inside the plaque ROI exceeding the 130 HU threshold. The second criterion was based on the generally used suggestion in calcium scoring schemes, that a threshold of more than 1 pixel for
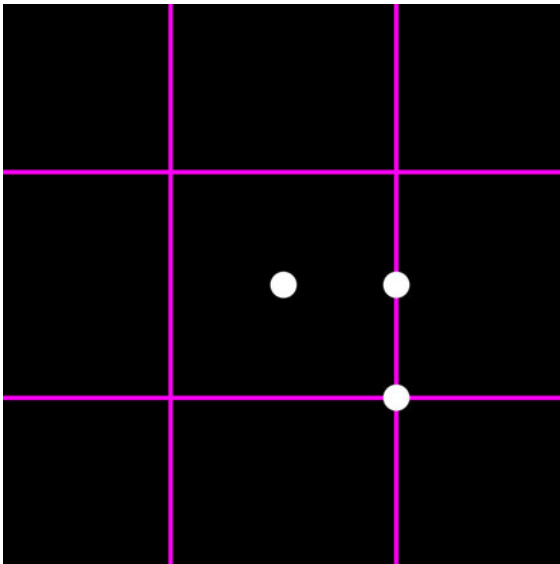
Fig. 2 The different positioning of calcification, at the image center (*1*), at the border between two image pixels (*2*), and at the border between four image pixels (*3*)

calcification is necessary to avoid false calcium detection due to noise [1].

Results

No noise

1. Minimal attenuation value of detectable calcification

The required attenuation value of 1, 2, 3, 5, and 10 pixel (5, 10, 15, 25, and 50 μm, respectively) diameter calcium granule(s) to be detectable by MicroCT and 64-MDCT is presented in Tables 2 and 3, respectively

(fixed diameter Ø rows). From all the detected calcium granule(s), only calcium granules with a diameter of at least 5 pixels (25 μm) which were detected by MicroCT, had an attenuation value within normal CT values range (−1,024 until +3,072 HU). Smaller calcifications required an unrealistically high attenuation value beyond this range to be detected. The simulation was stopped when a calcification with attenuation value >300,000 HU was still not detected.

2. Minimal size of detectable calcification

The required size of 2,000 HU calcium granule(s) to be detectable by MicroCT and 64-MDCT is presented in Tables 2 and 3, respectively (fixed attenuation rows). Using 1 pixel threshold, the smallest calcification detected by MicroCT and 64-MDCT were the ones positioned at the image pixel center with 20 and 175 μm diameter, respectively, with area overestimation of 5.8 and 6.7 times, respectively. Using >1 pixel threshold, the smallest calcification detected by MicroCT and 64-MDCT were the ones positioned at the border between two image pixels with 25 and 215 μm diameter, respectively, with area overestimation of 7.7 and 8.8 times, respectively.

The requirement of a calcification to be detected as 1 pixel, either by 64-MDCT or MicroCT, was constantly lower for calcification positioned at the image pixel center than the one positioned at the borders. However, to be detected as >1 pixel, the calcifications positioned at the image pixel center need the highest requirements.

With noise

The noise measured at the clinical 64-MDCT image sample was approximately 10 HU. If the same scan

Fig. 3 The photograph (*left*) and CT image (*right*) of the thorax phantom

Table 2 Detection prerequisites for MicroCT with no noise present

Fixed		Detection prerequisites of a calcification located at					
		Center		Border 2 pixels		Border 4 pixels	
		as 1 pixel	as >1 pixel	as 1 pixel	as >1 pixel	as 1 pixel	as >1 pixel
Diameter Ø	1 pixel	32,000 HU	65,000 HU	42,000 HU	44,000 HU	50,000 HU	52,000 HU
	2 pixels	8,000 HU	16,500 HU	10,500 HU	11,000 HU	12,500 HU	13,500 HU
	3 pixels	3,500 HU	7,000 HU	4,700 HU	5,000 HU	5,600 HU	5,900 HU
	5 pixels	1,300 HU	2,500 HU	1,800 HU	1,900 HU	2,100 HU	2,200 HU
	10 pixels	430 HU	800 HU	500 HU	600 HU	570 HU	600 HU
Attenuation	2,000 HU	4 pixel Ø	6 pixel Ø	N.A.	5 pixel Ø	N.A.	6 pixel Ø

N.A. data were not available since with the 1 pixel increment step, the calcification was directly detected as >1 pixel

Table 3 Detection prerequisites for 64-MDCT with no noise present

Fixed		Detection prerequisites of a calcification located at					
		Center		Border 2 pixels		Border 4 pixels	
		as 1 pixel	as >1 pixel	as 1 pixel	as >1 pixel	as 1 pixel	as >1 pixel
Diameter Ø	1 pixel	>300,000 HU	>300,000 HU	>300,000 HU	>300,000 HU	>300,000 HU	>300,000 HU
	2 pixels	>300,000 HU	>300,000 HU	>300,000 HU	>300,000 HU	>300,000 HU	>300,000 HU
	3 pixels	210,000 HU	>300,000 HU	>300,000 HU	>300,000 HU	>300,000 HU	>300,000 HU
	5 pixels	75,000 HU	130,000 HU	125,000 HU	135,000 HU	160,000 HU	170,000 HU
	10 pixels	18,000 HU	30,000 HU	32,000 HU	35,000 HU	40,000 HU	41,000 HU
Attenuation	2,000 HU	35 pixel Ø	49 pixel Ø	40 pixel Ø	43 pixel Ø	N.A.	45 pixel Ø

N.A. data were not available since with the 1 pixel increment step, the calcification was directly detected as >1 pixel

would have been performed at MicroCT spatial resolution without additional radiation dose, the noise level would have been at approximately 240 HU, which is too high for a diagnostic image. Inserting noise of that level to the Micro CT images will practically obscure any details, let alone the visualization of a small calcification. Therefore, the noise insertion was only performed to 64-MDCT images. Introduction of noise in the simulated 64-MDCT images changed the number of the detected calcification pixels, either by reducing the HU value of the detected calcification pixel so it went below the 130 HU threshold or by increasing the HU value of non-calcification pixel so it went above the 130 HU threshold (see Table 4).

One way to avoid being eliminated by the noise, the calcification pixel HU value needed to be above the noise level from the current threshold. Thus, the calcification needed to be at least 140 HU. Increasing the detection threshold accordingly, the detection requirements were updated as in Table 5.

Discussion

In this software simulation study, the attenuation value and size requirement of small calcifications necessary to be detectable by current clinical CT systems (represented by 64-MDCT), were systematically investigated. Very small calcifications (≤50 μm diameter) needed an unrealistically high attenuation value, while calcifications of a realistic attenuation value had to have at least a 215 μm (0.215 mm) diameter. Calcifications with a size or attenuation value below these requirements would simply be blurred out due to partial volume effects.

Contrast-enhanced coronary CT angiography examinations have been widely used for coronary artery disease examination, both for coronary lumen and wall assessment [33–38]. However, coronary calcification quantification based on non-contrast-enhanced coronary CT remains a solid assessment tool for predicting coronary event risk [2–4]. It has been associated with total plaque burden [39].

Table 4 The change of detected calcification pixels at 64-MDCT with noise present

Fixed		Change in the detected pixels					
		Center		Border 2 pixels		Border 4 pixels	
		as 1 pixel	as >1 pixel	as 1 pixel	as >1 pixel	as 1 pixel	as >1 pixel
Diameter Ø	1 pixel	N.A.	N.A.	N.A.	N.A.	N.A.	N.A.
	2 pixels	N.A.	N.A.	N.A.	N.A.	N.A.	N.A.
	3 pixels	0	N.A.	N.A.	N.A.	N.A.	N.A.
	5 pixels	0	0	−1	−1	+	+1
	10 pixels	0	−1	−1	−1	+1	0
Attenuation	2,000 HU	−1	−1	0	0	N.A.	−1

N.A. data were not available since the simulation was not performed at this setting

Table 5 Detection prerequisites for 64-MDCT with noise present

Fixed		Detection prerequisites of a calcification located at					
		Center		Border 2 pixels		Border 4 pixels	
		as 1 pixel	as > 1 pixel	as 1 pixel	as > 1 pixel	as 1 pixel	as > 1 pixel
Diameter Ø	1 pixel	>300,000 HU	>300,000 HU	>300,000 HU	>300,000 HU	>300,000 HU	>300,000 HU
	2 pixels	>300,000 HU	>300,000 HU	>300,000 HU	>300,000 HU	>300,000 HU	>300,000 HU
	3 pixels	250,000 HU	>300,000 HU	>300,000 HU	>300,000 HU	290,000 HU	>300,000 HU
	5 pixels	85,000 HU	150,000 HU	145,000 HU	155,000 HU	185,000 HU	190,000 HU
	10 pixels	20,000 HU	35,000 HU	37,000 HU	39,000 HU	46,000 HU	47,000 HU
Attenuation	2,000 HU	38 pixel Ø	53 pixel Ø	43 pixel Ø	46 pixel Ø	45 pixel Ø	48 pixel Ø

Although extensive calcifications are associated with more stable plaques [40–42], they are frequently found in ruptured plaques according to a histopathology study on victims of sudden coronary death [43]. However, speckled calcifications are more commonly associated with ruptured and vulnerable plaques than diffuse calcification [44]. Above all, mixed plaques with predominantly non-calcifying component are associated with acute coronary syndromes [40]. Some studies have shown that absence of coronary calcium can 100% rule out the presence of significant CAD on CT angiography in symptomatic patients [10, 12]. Other studies have found contradicting results, with significant stenoses in up to 7% of patients with zero or very low calcium score [11, 13, 14]. The sensitivity of the CT technique applied may play an important role. Furthermore, dependency of coronary calcification quantification on acquisition mode, quantification algorithm, and vendor were reported [45]. A study comparing coronary calcification quantifications by multiple 64-MDCT scanners from two different vendors addressed the inability to detect all small and less dense calcifications by all 64-MDCT scanners [16]. One pathological study reported a few missed calcifications by MDCT [46]. Another pathological study supports our findings, describing the limitations of 64-MDCT in detecting small calcifications and also the overestimation of the detected calcifications area [47]. A recent clinical study reported missed small calcifications by contrast-enhanced MDCT and confirmed the limited spatial resolution as the main cause instead of the lumen contrast-enhancement influence [48].

Stary et al. [49] noted that calcifications could be observed at the same time as the plaques reached an advanced stage. However, a recent finding shows that micro-calcifications (sized 1–10 μm) are already present in an early type of atherosclerotic plaque, indicating the possibility of calcium to be a marker for early development hereof atherosclerosis [50]. Vengrenyuk et al. [51] hypothesized that micro-calcifications in the thin fibrous cap covering a lipid

pool could destabilize the plaque to the point of becoming rupture-prone. However, for these micro-calcifications to be detectable by 64-MDCT, an unrealistically high attenuation value is needed. A MicroCT is necessary to detect these micro-calcifications, while a macro CT, such as the 64-MDCT, is limited to larger coronary calcifica-tions. Langheinrich et al. [52] showed that MicroCT with 12 μm spatial resolution could visualize small (<100 μm^2 or ~ 10 μm diameter) and very dense iron deposits. However, as the spatial resolution decreased, these iron deposits became blurred out and at a spatial resolution of around 50 μm, they started to be completely blurred out. This concurred with our results in a MicroCT of similar spatial resolution (48 μm), in which calcification of a similar size (2-pixel or 10 μm diameter) and a similar attenuation value as the iron deposits started to be detected (see Table 2).

The presence of noise influenced the detectability of small calcifications, affecting more than half of the detected calcifications by 64-MDCT. The effect of noise may be avoided by setting a higher HU threshold for calcification detection. However, it will also mean that only larger and denser calcification can be detected, while smaller and less dense calcification will be missed. No noise evaluation was performed for the MicroCT images as the increased noise level will severely limit further evaluation.

The current developments in CT, in term of spatial resolution, are marked by the introduction of a new 230 μm-spatial resolution CT system [53] and the emerging technology of a 200 μm-spatial resolution flat panel CT system [47]. Higher spatial resolution may allow CT systems to detect smaller calcifica-tions, but the main challenge lies in dealing with the accompanying higher noise level while keeping the radiation dose comparable to clinical settings [32, 52]. Technological advances such as the iterative reconstruction algorithm may offer a solution to this problem [53]. So far in vivo modalities that may visualize ultrasmall calcifications are invasive modal-ities such as intravascular ultrasound (IVUS) and optical coherence tomography (OCT) [54]. However, invasive modalities can only be applied in selected high-risk patient groups.

The calcification quantification method used in this study follows the commonly accepted threshold-based calcification quantification method [1]. The method is simple yet effective, as has been shown in many studies. However, the usage of a fixed threshold to quantify coronary calcification may not properly take into account the true volume of calcification. Advanced new image post-processing techniques may improve the current established calcification quantification method.

This study does not simulate different types of vessel remodeling as the type of remodeling should not have any influence on the visualization of small calcifications. However, it is of importance in non-calcified plaque attenuation value measurements as plaque, which causes positive remodeling, had a low attenuation value, which is associated with higher vulnerability [55]. The lack of physical CT scanning properties in this study is compensated by the fact that software simulation can systematically adjust individually influencing factors while mimicking the technical settings of a CT system as closely as possible. Due to the simulation software limitation, however, some parameters, such as the X-ray source-detector geometry, can only be approximated. This also applies to properties such as the reconstruction filter details, since these are not always disclosed by the CT vendor. The analysis is limited to two dimensional (2D) images also because of the limita-tion of the simulation software. However, since calcification measurement is commonly assessed based on its area [1, 39, 47], our result should sufficiently show 64-MDCT limitations in detecting calcification. Also it should be noted that calcification is a three-dimensional (3D) object and its volume comparison to the image voxel size can play a role in the partial volume effect. Although cardiac motion has been reported to affect the coronary calcium score [56], the effect of motion on the detection of small calcifications was excluded in this current study. However, it is expected that including motion will increase the size and attenuation value require-ment of a small calcification to be detectable by 64-MDCT. The ideal noiseless and motionless envi-ronment gave us the opportunity to focus our study on the relation between spatial resolution and the detectability of a small calcification. Future work should incorporate all these considerations to provide even more solid proof on how small calcifications may be missed by 64-MDCT or current clinical CT systems in general.

In conclusion, 64-MDCT is only able to detect coronary calcifications with minimal diameter of 215 μm, which is approximately 40 times the smallest reported calcium granule size. Consequently, early onset of calcification in coronary plaque indicating early progression of disease and increased coronary risk to the patient will go undetected when using a clinical CT system; and a zero calcium score can not exclude the presence of coronary calcification.

References

1. Agatston AS, Janowitz WR, Hildner FJ, Zusmer NR, Viamonte M Jr, Detrano R (1990) Quantification of coronary artery calcium using ultrafast computed tomography. J Am Coll Cardiol 15:827–832
2. Arad Y, Goodman KJ, Roth M, Newstein D, Guerci AD (2005) Coronary calcification, coronary disease risk factors, C-reactive protein, and atherosclerotic cardiovascular disease events the St. Francis Heart Study. J Am Coll Cardiol 46:158–165
3. Greenland P, LaBree L, Azen SP, Doherty TM, Detrano RC (2004) Coronary artery calcium score combined with Framingham score for risk prediction in asymptomatic individuals. Jama 291:210–215
4. Vliegenthart R, Oudkerk M, Hofman A, Oei HHS, van Dijck W, van Rooij FJA, Witteman J (2005) Coronary calcification improves cardiovascular risk prediction in the elderly. Circulation 112:572–577
5. Greenland P, Bonow RO, Brundage BH, Budoff MJ, Eisenberg MJ, Grundy SM, Lauer MS, Post WS, Raggi P, Redberg RF (2007) Coronary artery calcium scoring: ACCF/AHA 2007 clinical expert consensus document on coronary artery calcium scoring by computed tomography in global cardiovascular risk assessment and in evaluation of patients with chest pain. J Am Coll Cardiol 49:378–402
6. Oudkerk M, Stillman AE, Halliburton SS, Kalender WA, Mohlenkamp S, McCollough CH, Vliegenthart R, Shaw LJ, Stanford W, Taylor AJ, van Ooijen PM, Wexler L, Raggi P (2008) Coronary artery calcium screening: current status and recommendations from the European society of cardiac radiology and North American society for cardiovascular imaging. Int J Cardiovasc Imaging 24:645–671
7. Oudkerk M, Stillman AE, Halliburton SS, Kalender WA, Mohlenkamp S, McCollough CH, Vliegenthart R, Shaw LJ, Stanford W, Taylor AJ, van Ooijen PM, Wexler L, Raggi P (2008) Coronary artery calcium screening: current status and recommendations from the European society of cardiac radiology and North American society for cardiovascular imaging. Eur Radiol 18:2785–2807
8. Blaha M, Budoff MJ, Shaw LJ, Khosa F, Rumberger JA, Berman D, Callister T, Raggi P, Blumenthal RS, Nasir K (2009) Absence of coronary artery calcification and all-cause mortality. JACC Cardiovasc Imaging 2:692–700
9. Sarwar A, Shaw LJ, Shapiro MD, Blankstein R, Hoffman U, Cury RC, Abbara S, Brady TJ, Budoff MJ, Blumenthal RS (2009) Diagnostic and prognostic value of absence of coronary artery calcification. JACC Cardiovasc Imaging 2:675–688
10. Cheng VY, Lepor NE, Madyoon H, Eshaghian S, Naraghi AL, Shah PK (2007) Presence and severity of noncalcified coronary plaque on 64-slice computed tomographic coronary angiography in patients with zero and low coronary artery calcium. Am J Cardiol 99:1183–1186
11. Choi EK, Choi SI, Rivera JJ, Nasir K, Chang SA, Chun EJ, Kim HK, Choi DJ, Blumenthal RS, Chang HJ (2008) Coronary computed tomography angiography as a screening tool for the detection of occult coronary artery disease in asymptomatic individuals. J Am Coll Cardiol 52:357–365
12. Ho JS, FitzGerald SJ, Stolfus LL, Wade WA, Reinhardt DB, Barlow CE, Cannaday JJ (2008) Relation of a coronary artery calcium score higher than 400 to coronary stenoses detected using multidetector computed tomography and to traditional cardiovascular risk factors. Am J Cardiol 101:1444–1447
13. Kelly JL, Thickman D, Abramson SD, Chen PR, Smazal SF, Fleishman MJ, Lingam SC (2008) Coronary CT angiography findings in patients without coronary calcification. Am J Roentgenol 191:50–55
14. Rubinshtein R, Gaspar T, Halon DA, Goldstein J, Peled N, Lewis BS (2007) Prevalence and extent of obstructive coronary artery disease in patients with zero or low calcium score undergoing 64-slice cardiac multidetector computed tomography for evaluation of a chest pain syndrome. Am J Cardiol 99:472–475
15. Greenland P, Bonow RO (2008) How low-risk is a coronary calcium score of zero?: the importance of conditional probability. Circulation 117:1627–1629
16. Dijkstra H, Greuter MJW, Groen JM, Vliegenthart-Proenτa R, Renema KJWK, de Lange F, Oudkerk M (2010) Coronary calcium mass scores measured by identical 64-slice MDCT scanners are comparable: a cardiac phantom study. Int J Cardiovasc Imaging 26:89–98
17. Olszewski ME, Wahle A, Khullar D, Subramanyan K, Sonka M (2005) A study investigating automated quantitative analyses of coronary multidetector computed tomography images. Proceedings of SPIE 5746:214–222
18. Rosenberg K (2001) CTSim-the open source computed tomography simulator. URL http://www.ctsim.org/. Accessed 14 May 2009

19. Stary HC (2001) The development of calcium deposits in atherosclerotic lesions and their persistence after lipid regression. Am J Cardiol 88:16E–19E

20. Berglund H, Luo H, Nishioka T, Fishbein MC, Eigler NL, Tabak SW, Siegel RJ (1997) Highly localized arterial remodeling in patients with coronary atherosclerosis: an intravascular ultrasound study. Circulation 96:1470–1476

21. de Weert TT, Ouhlous M, Meijering E, Zondervan PE, Hendriks JM, van Sambeek MR, Dippel DW, van der Lugt A (2006) In vivo characterization and quantification of atherosclerotic carotid plaque components with multidetector computed tomography and histopathological correlation. Arterioscler Thromb Vasc Biol 26:2366–2372

22. Gorter PM, van Lindert ASR, de Vos AM, Meijs MFL, van der Graaf Y, Doevendans PA, Prokop M, Visseren FLJ (2008) Quantification of epicardial and peri-coronary fat using cardiac computed tomography; reproducibility and relation with obesity and metabolic syndrome in patients suspected of coronary artery disease. Atherosclerosis 197:896–903

23. Gradus-Pizlo I, Bigelow B, Mahomed Y, Sawada SG, Rieger K, Feigenbaum H (2003) Left anterior descending coronary artery wall thickness measured by high-frequency transthoracic and epicardial echocardiography includes adventitia. Am J Cardiol 91:27–32

24. Haraguchi K, Houkin K, Koyanagi I, Nonaka T, Baba T (2008) Evaluation of carotid plaque composition by computed tomographic angiography and black blood magnetic resonance images. Minim Invasive Neurosurg 51:91–94

25. Noguchi K, Seto H, Kamisaki Y, Tomizawa G, Toyoshima S, Watanabe N (2000) Comparison of fluid-attenuated inversion-recovery MR imaging with CT in a simulated model of acute subarachnoid hemorrhage. Am J Neuroradiol 21:923–927

26. Walker LJ, Ismail A, McMeekin W, Lambert D, Mendelow AD, Birchall D (2002) Computed tomography angiography for the evaluation of carotid atherosclerotic plaque: correlation with histopathology of endarterectomy specimens. Stroke 33:977–981

27. Wheeler GL, Shi R, Beck SR, Langefeld CD, Lenchik L, Wagenknecht LE, Freedman BI, Rich SS, Bowden DW, Chen MY (2005) Pericardial and visceral adipose tissues measured volumetrically with computed tomography are highly associated in type 2 diabetic families. Invest Radiol 40:97–101

28. Wintermark M, Jawadi SS, Rapp JH, Tihan T, Tong E, Glidden DV, Abedin S, Schaeffer S, Acevedo-Bolton G, Boudignon B, Orwoll B, Pan X, Saloner D (2008) High-resolution CT imaging of carotid artery atherosclerotic plaques. Am J Neuroradiol 29:875–882

29. Stary HC (2000) Natural history of calcium deposits in atherosclerosis progression and regression. Z Kardiol 89(Suppl 2):28–35

30. Galonska M, Ducke F, Kertesz-Zborilova T, Meyer R, Guski H, Knollmann FD (2008) Characterization of atherosclerotic plaques in human coronary arteries with 16-slice multidetector row computed tomography by analysis of attenuation profiles. Acad Radiol 15:222–230

31. Joemai RMS, Geleijns J, Veldkamp WJH (2010) Development and validation of a low dose simulator for computed tomography. Eur Radiol 20:958–966

32. Brooks RA, Di Chiro G (1976) Statistical limitations in X-ray reconstructive tomography. Med Phys 3:237–240

33. Achenbach S, Ulzheimer S, Baum U (2000) Noninvasive coronary angiography by retrospectively ECG-gated multislice spiral CT. Circulation 102:2823–2828

34. Achenbach S, Giesler T, Ropers D, Ulzheimer S, Derlien H, Schulte C, Wenkel E, Moshage W, Bautz W, Daniel WG, Kalender WA, Baum U (2001) Detection of coronary artery stenoses by contrast-enhanced, retrospectively electrocardiographically-gated, multislice spiral computed tomography. Circulation 103:2535–2538

35. Inoue F, Sato Y, Matsumoto N, Tani S, Uchiyama T (2004) Evaluation of plaque texture by means of multislice computed tomography in patients with acute coronary syndrome and stable angina. Circ J 68:840–844

36. Moselewski F, Ropers D, Pohle K, Hoffmann U, Ferencik M, Chan RC, Cury RC, Abbara S, Jang I, Brady TJ (2004) Comparison of measurement of cross-sectional coronary atherosclerotic plaque and vessel areas by 16-slice multidetector computed tomography versus intravascular ultrasound. Am J Cardiol 94:1294–1297

37. Nikolaou K, Becker CR, Muders M, Babaryka G, Scheidler J, Flohr T, Loehrs U, Reiser MF, Fayad ZA (2004) Multidetector-row computed tomography and magnetic resonance imaging of atherosclerotic lesions in human ex vivo coronary arteries. Atherosclerosis 174:243–252

38. Schoenhagen P, Murat Tuzcu E, Stillman AE, Moliterno DJ, Halliburton SS, Kuzmiak SA, Kasper JM, Magyar WA, Lieber ML, Nissen SE (2003) Non-invasive assessment of plaque morphology and remodeling in mildly stenotic coronary segments: comparison of 16-slice computed tomography and intravascular ultrasound. Coron Artery Dis 14:459–462

39. Sangiorgi G, Rumberger JA, Severson A, Edwards WD, Gregoire J, Fitzpatrick LA, Schwartz RS (1998) Arterial calcification and not lumen stenosis is highly correlated with atherosclerotic plaque burden in humans: a histologic study of 723 coronary artery segments using nondecalcifying methodology. J Am Coll Cardiol 31:126–133

40. Feuchtner G, Postel T, Weidinger F, Frick M, Alber H, Dichtl W, Jodocy D, Mallouhi A, Pachinger O, Zur Nedden D, Friedrich GJ (2008) Is there a relation between non-calcifying coronary plaques and acute coronary syndromes? A retrospective study using multislice computed tomography. Cardiology 110:241–248

41. Pundziute G, Schuijf JD, Jukema JW, Decramer I, Sarno G, Vanhoenacker PK, Boersma E, Reiber JH, Schalij MJ, Wijns W, Bax JJ (2008) Evaluation of plaque characteristics in acute coronary syndromes: non-invasive assessment with multi-slice computed tomography and invasive evaluation with intravascular ultrasound radiofrequency data analysis. Eur Heart J 29:2373–2381

42. Schuijf JD, Beck T, Burgstahler C, Jukema JW, Dirksen MS, de Roos A, van der Wall EE, Schroeder S, Wijns W, Bax JJ (2007) Differences in plaque composition and distribution in stable coronary artery disease versus acute coronary syndromes; non-invasive evaluation with multi-slice computed tomography. Acute Card Care 9:48–53

43. Burke AP, Taylor A, Farb A, Malcom GT, Virmani R (2000) Coronary calcification: insights from sudden coronary death victims. Z Kardiol 89:49–53

44. Burke AP, Weber DK, Kolodgie FD, Farb A, Taylor AJ, Virmani R (2001) Pathophysiology of calcium deposition in coronary arteries. Herz 26:239–244

45. Greuter MJ, Dijkstra H, Groen JM, Vliegenthart R, de Lange F, Renema WK, de Bock GH, Oudkerk M (2007) 64 slice MDCT generally underestimates coronary calcium scores as compared to EBT: a phantom study. Med Phys 34:3510–3519

46. Becker CR, Nikolaou K, Muders M, Babaryka G, Crispin A, Schoepf UJ, Loehrs U, Reiser MF (2003) Ex vivo coronary atherosclerotic plaque characterization with multi-detector-row CT. Eur Radiol 13:2094–2098

47. Sarwar A, Rieber J, Mooyaart EAQ, Seneviratne SK, Houser SL, Bamberg F, Raffel OC, Gupta R, Kalra MK, Pien H (2008) Calcified plaque: measurement of area at thin-section flat-panel CT and 64-section multidetector CT and comparison with histopathologic findings 1. Radiology 249:301–306

48. van der Giessen A, Gijsen F, Wentzel J, Jairam P, van Walsum T, Neefjes L, Mollet N, Niessen W, van de Vosse F, de Feyter P, van der Steen A (2010) Small coronary calcifications are not detectable by 64-slice contrast enhanced computed tomography. Int J Cardiovasc Imaging 27:143–152

49. Stary HC, Chandler AB, Dinsmore RE, Fuster V, Glagov S, Insull W Jr, Rosenfeld ME, Schwartz CJ, Wagner WD, Wissler RW (1995) A definition of advanced types of atherosclerotic lesions and a histological classification of atherosclerosis. A report from the committee on vascular lesions of the council on arteriosclerosis, American heart association. Circulation 92:1355–1374

50. Roijers RB, Dutta RK, Cleutjens JP, Mutsaers PH, de Goeij JJ, van der Vusse GJ (2008) Early calcifications in human coronary arteries as determined with a proton microprobe. Anal Chem 80:55–61

51. Vengrenyuk Y, Carlier S, Xanthos S, Cardoso L, Ganatos P, Virmani R, Einav S, Gilchrist L, Weinbaum S (2006) A hypothesis for vulnerable plaque rupture due to stress-induced debonding around cellular microcalcifications in thin fibrous caps. Proc Natl Acad Sci USA 103:14678–14683

52. Langheinrich AC, Kampschulte M, Cröâmann C, Moritz R, Rau WS, Bohle RM, Ritman EL (2009) Role of Computed Tomography Voxel Size in Detection and Discrimination of Calcium and Iron Deposits in Atherosclerotic Human Coronary Artery Specimens. J Comput Assist Tomogr 33: 517–522

53. Fan J, Dong F, Sainath P, Hsieh J, Tang X, Toth T, Li B, Crandall P, Senzig R, Dixon A (2009) Image quality evaluation of a lightspeed CT750 HD computed tomography system. In: Samei E, Hsieh J (eds) Medical Imaging 2009: Physics of Medical Imaging. SPIE Press, Bellingham, USA, pp 72584S-1–72584S-8

54. Weinbaum S, Vengrenyuk Y, Cardoso L, Parra L, Carlier S, Xanthos S (2008) SYSTEM AND METHOD FOR IN VIVO IMAGING OF BLOOD VESSEL WALLS TO DETECT MICROCALCIFICATIONS. US Patent US/2008/0091105 A1, filed Sep 25, 2007 and issued Apr 17, 2008

55. Schmid M, Pflederer T, Jang IK, Ropers D, Sei K, Daniel WG, Achenbach S (2008) Relationship between degree of remodeling and CT attenuation of plaque in coronary atherosclerotic lesions: an in vivo analysis by multi-detector computed tomography. Atherosclerosis 197:457–464

56. Funabashi N, Koide K, Mizuno N, Nagamura K, Ochi S, Yanagawa N, Okamoto Y, Uno K, Komuro I (2006) Influence of heart rate on the detectability and reproducibility of multislice computed tomography for measuring coronary calcium score using a pulsating calcified mock-vessel in comparison with electron beam tomography. Int J Cardiol 113:113–117